# Flood Detection and Analysis: A Case Study of the Akosombo Dam Spillage Event 2023

**BLEBOO Angela Bubune & KPONOR Mark Kofi, GHANA**

**Keywords:** Flood Detection, Remote Sensing, Google Earth Engine, Sentinel-1 SAR, Hazard Mapping

## SUMMARY

The Akosombo Dam spillage in September–October 2023 triggered extensive flooding along the Volta River, displacing over 31,000 people and causing severe damage to croplands, urban areas, and infrastructure. This study leverages Sentinel-1 Synthetic Aperture Radar (SAR) data and Google Earth Engine (GEE) to analyze flood dynamics, assess affected land cover, and develop a flood hazard map for improved disaster preparedness. Multi-temporal SAR analysis was employed to detect inundation extent across key dates, with the highest flood coverage recorded at 4,110 hectares on October 16. The methodology involved preprocessing SAR images through speckle filtering, water masking, and threshold-based classification to accurately delineate flood extent. The impact assessment was conducted by overlaying flood maps with ESA WorldCover landcover data to quantify losses in cropland and urban areas. Additionally, flood hazard mapping incorporated topographic factors such as elevation, proximity to water bodies, and vegetation indices to classify risk zones. Safe havens were identified using proximity analysis to assist in evacuation planning. The study also applied post-processing techniques, including connectivity analysis and slope masking, to refine flood extent detection and minimize classification errors. The results underscore the effectiveness of remote sensing for flood detection and risk mapping, offering crucial insights for policymakers, emergency responders, and urban planners. The study highlights the need for enhanced flood monitoring, real-time early warning systems, and resilient infrastructure development to mitigate future flood risks in Ghana. The findings contribute to disaster management frameworks by demonstrating how satellite-based geospatial analysis can improve flood response and long-term risk reduction strategies.

## 1. INTRODUCTION

Since its completion in 1965, Ghana's massive hydroelectric dam on the Volta River has served as a pillar of the country's energy infrastructure. The dam is located on the river. The reservoir of the dam, which is mainly intended for the production of power, covers an area of around 8,500 square kilometres and is essential for the Volta Basin's agriculture, fishery, and urban supply. Controlled by the Volta River Authority (VRA), the dam is essential to maintaining the stability of Ghana's electrical system and promoting regional economic growth. September 2023 saw extremely heavy rainfall in Ghana's Lower Volta area, which led to the Akosombo Dam surpassing its operational limit of 277.54 feet. The VRA began a controlled leak on September 15, 2023, to lessen potential risks to the dam's structural integrity. The settlements downstream saw a minimal impact from the leak when it first started since it was controlled gradually. But, as the wet season went on, reservoir levels increased, necessitating the opening of six spillage gates by October 10, 2023, to contain the issue. The increased water discharge led to severe flooding downstream, particularly affecting the districts of North and Central Tongu, including the towns of Mepe, Battor, Sogakope, Mafi, Adidome, and Ada (*The Akosombo Dam Spillage | UNICEF Ghana*, 2023). Over 31,000 residents were displaced, marking the event as the most severe flooding in the region's history (Miescher, 2023). Although there were no reported fatalities, homes, infrastructure, and agricultural lands suffered extensive damage. Concerns have been voiced over the flood's potential effects on the local ecosystems and communities from an environmental, social, and economic standpoint. Houses are submerged, while crops and infrastructure have suffered severe material damage. Two hydropower dams at Akosombo and Kpong overflowed, destroying crops and forcing the closure of schools. The floods damaged Farmlands and residential buildings, which also seriously interrupted the delivery of essential utilities, especially electricity and water. The Volta River Authority (VRA) provides crowded living conditions in schools and other institutions where the displaced people are kept due to a lack of housing. The recent flooding caused by the Akosombo Dam's overflow has highlighted a critical issue: the dam's current management practices and infrastructure are insufficient to handle extreme weather events. This inadequacy has led to the displacement of thousands of residents, significant damage to homes and farmland, and disruption of local economies. The core problem is the lack of an effective flood management and early warning system, intensified by inadequate dam infrastructure maintenance. While immediate flood mapping and disaster response efforts were essential, there remains a critical gap in understanding the long-term implications and effective management strategies for dam spillage-induced floods. The primary objective of this study is to assess the flood extent and impact of the Akosombo Dam spillage using remote sensing and GIS. Specifically mapping the flood extent using Sentinel-1 SAR imagery, evaluating the impact of flooding on croplands and urban areas and developing a flood hazard map to inform future flood mitigation strategies. Remote sensing and GIS offer significant advantages in flood monitoring by providing near real-time, high-resolution data for decision-making. This study contributes to the development of more effective flood management strategies in Ghana by leveraging cloud-based geospatial analysis tools such as Google Earth Engine (GEE). The findings will support policymakers, disaster response agencies, and local authorities in designing adaptive measures to mitigate future flood risks.

## 2. METHODOLOGY

### 2.1 Study Area

The study focuses on the Volta River Basin, covering affected districts such as North and Central Tongu. The region experiences seasonal rainfall, making it prone to flooding, especially during dam spillages.

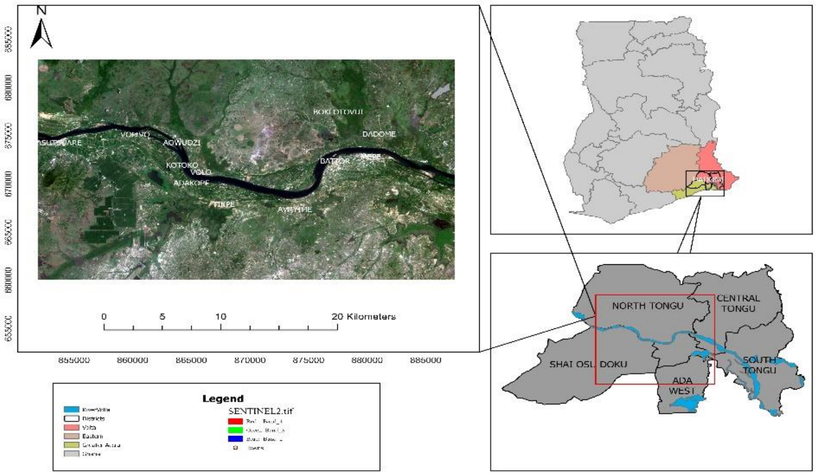


### 2.2 Data Collection

| DataSets | Period | Resolution | Source/Provider | Purpose | GEE assess Address |
|---|---|---|---|---|---|
| Sentinel-1 SAR GRD | September-October 2023 | 10m | European Union/ESA/Copernicus | To extract flood extent and flood-affected areas | ee.ImageCollection ("COPERNICUS/S1_GRD") |
| NASA SRTM Digital Elevation | | 30m | NASA / USGS / JPL-Caltech | Used to derive the topographic features of the study area | ee.Image("USGS/SRTMGL1_003") |
| Copernicus Global Land Cover Layers | 2021 | 10 | ESA/VITO/Brockmann Consult/CS/GAMMA Remote Sensing/IIASA/WUR | LULC Map for impact a | ee.ImageCollection ("ESA/WorldCover/v100") |
| Harmonized Sentinel-2 MSI | September-October 2023 | 10 | European Union/ESA/Copernicus | Essential for calculating flood hazard | ee.ImageCollection ("COPERNICUS/S2_SR_HARMONIZED") |

### 2.3 Data Processing and Analysis

The preprocessing of Sentinel-1 SAR images involved several critical steps to ensure data suitability for flood detection. Image selection was refined by filtering images based on the Interferometric Wide Swath (IW) mode, chosen for its extensive area coverage while maintaining a high spatial resolution of 10 meters. This mode is particularly effective for monitoring large-scale flood events due to its balance between spatial resolution and coverage (Vanama et al., 2020). Furthermore, data were filtered by orbit properties, selecting only ascending (northbound) passes to maintain consistency in viewing geometry and minimize potential artifacts, such as foreshortening and layover, which are more pronounced in descending passes. Single-polarization (VH) was employed to enhance water detection, as VH polarization is more sensitive to surface water, which reflects this polarization differently compared to land, thus improving the ability to distinguish flooded areas from surrounding terrain. The data collection period spanned from September 1, 2023, to October 31, 2023, ensuring comprehensive temporal coverage before, during, and after flood events. This temporal filtering was crucial for capturing pre-flood, during-flood, and post-flood conditions, documenting the dynamics of the flooding event over time. This step ensured that all subsequent analyses were confined to the region of interest, increasing the accuracy and relevance of the results.
A multi-temporal analysis approach was employed to detect flooded areas by comparing SAR images from different dates. The first step in this approach was image mosaicking, where multiple images from the same date were combined to form a single mosaic. This process ensured complete spatial coverage and created seamless coverage of the study area for each date, which is crucial for accurate flood mapping over large areas. To reduce the noise inherent in SAR images, known as speckle, which can obscure flood signals, speckle filtering was applied. A focal mean filter with a 30-meter radius was used to smooth the images while preserving essential details, which is a common technique to enhance the interpretability of SAR data. (Ali et al., 2018) argue that effective speckle filtering is necessary to maintain the balance between noise reduction and detail preservation, which is crucial for detecting subtle changes in flood extent. Difference calculation was then performed to identify changes in surface water extent by comparing SAR images from different dates. Different images were computed by dividing post-event images by pre-event images, highlighting areas with significant changes in backscatter, indicative of flooding. This method, known as Logarithmic differencing, is effective for detecting subtle changes in water bodies that may be missed using other techniques. Both (Notti et al., 2018; Schlaffer et al., 2017) agree on the utility of logarithmic differencing for enhancing the detectability of flooded areas by amplifying changes in backscatter that are characteristic of water presence. Thresholding was used to classify pixels as flooded or non-flooded based on the difference images. An upper threshold value of 1.25 was determined by analyzing the histogram of difference images. This threshold was chosen to maximize the detection of true flood pixels while minimizing false positives, establishing a cut-off value that distinguished between flooded and non-flooded areas. Pixels with values exceeding the threshold were classified as flooded, resulting in a binary image that highlighted flooded areas and created a binary flood map.

Post-processing steps were applied to refine the flood maps and improve accuracy. Connectivity analysis was conducted, calculating pixel connectivity and retaining only clusters of pixels connected by more than eight neighbours. This step is crucial for removing isolated pixels that are unlikely to represent true flooded areas, thereby reducing noise and improving the accuracy of flood extent maps. Slope masking was also applied. Using the Shuttle Radar Topography Mission (SRTM) Digital Elevation Model (DEM), areas with slopes greater than 5% were masked out. This step excluded pixels in areas with significant slopes, as these regions are less likely to be flooded, thereby enhancing the reliability of flood detection in flatter areas prone to inundation. Finally, water masking was performed using the European Space Agency (ESA) land cover map to identify and remove permanent water bodies from the flood maps. This differentiation between temporary flooded areas and permanent water bodies is essential for accurately representing flood dynamics and for subsequent flood impact assessments (Podest & Mccartney, 2019).

### 2.4 Impact Assessment

The inundation extent was calculated by converting binary flood maps into physical areas and summing flooded pixels to determine the total flooded area in hectares. To assess the impact on cropland and urban areas, the ESA land cover map was used to extract relevant land classes. A binary cropland mask was created to isolate agricultural land, which was then overlaid with flood extent maps to identify affected areas. The total flooded cropland was quantified by summing the intersecting pixels, providing a measure of agricultural losses. The same methodology was applied to urban areas, generating a binary urban mask and overlaying it with flood maps to determine the extent of urban flooding. This approach ensured a systematic assessment of flood damage, offering valuable insights into the impact on both agricultural production and infrastructure.

### 2.5 Flood Hazard

A Flood Hazard Assessment was implemented. This step involved isolating water bodies within the ESA Land Cover Data. Classes corresponding to water (class values 80 and 200) were identified using a masking technique, essential for delineating water bodies as key factors in flood modelling. The distance from these water bodies was calculated using the fast distance transform algorithm, providing a spatial representation of proximity to water bodies.

To refine the flood hazard assessment, permanent water bodies identified within the Land Cover Data dataset were excluded from distance calculations. This exclusion was necessary to prevent skewing the results, as permanent water bodies exhibit different flood dynamics compared to temporary water accumulation areas. The resulting distance data was reclassified into hazard scores, with closer proximity to water bodies indicating higher flood risk.

Distance > 1000 meters: Score of 1, 750 -1000 meters: Score of 2, 500 - 750 meters: Score of 3, 250 - 500 meters: Score of 4, < 250 meters: Score of 5.

Elevation data from the Shuttle Radar Topography Mission (SRTM) played a crucial role in the analysis. Lower elevations, typically associated with higher flood risk, were categorized into various risk levels based on specific thresholds. This elevation scoring system allowed for a nuanced understanding of how terrain height influences flood susceptibility.

Elevation < 5%: Score of 5, 5% - 10%: Score of 4, 10% - 15%: Score of 3, 15% - 20%: Score of 2, > 20%: Score of 1.

The study also utilized the Topographic Position Index (TPI), calculated using SRTM data, to measure the relative elevation of a point compared to its surroundings. This metric helped identify features such as valleys or ridges, which have distinct flood dynamics. TPI values were scored based on deviation from the mean elevation, with significant deviations indicating higher flood risk. Additionally, the study incorporated vegetation and wetness indices derived from the Sentinel-2 dataset. The Normalized Difference Vegetation Index (NDVI) assessed vegetation cover, which influences water absorption and runoff, with areas of low vegetation cover indicating higher flood risk. The Normalized Difference Water Index (NDWI) evaluated surface water presence, identifying areas with persistent wetness that could exacerbate flooding.

The combination of these indices distance from water, elevation, TPI, NDVI, and NDWI culminated in a comprehensive flood hazard score. The scores were normalized to a scale of 1 to 5, with 5 indicating the highest risk. This scoring system allowed for clear visualization and interpretation of flood risk across the study area.

Flood hazard score > 15%: Score of 5, 10% - 15%: Score of 4, 5% - 10: Score of 3, 0% - 5%: Score of 2, < 0%: Score of 1.

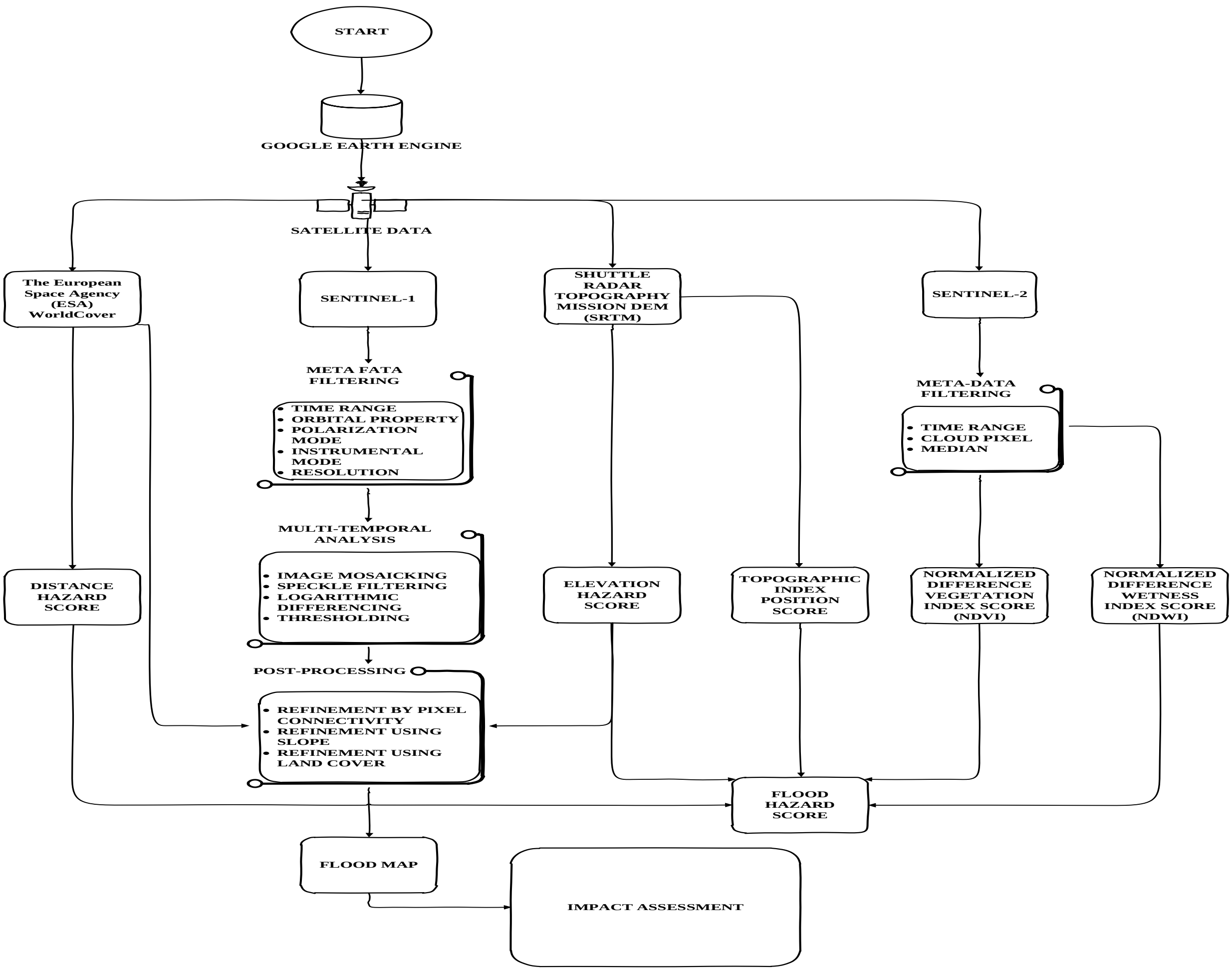

# 4. RESULTS AND ANALYSIS

## 4.1 Flood Extent Mapping

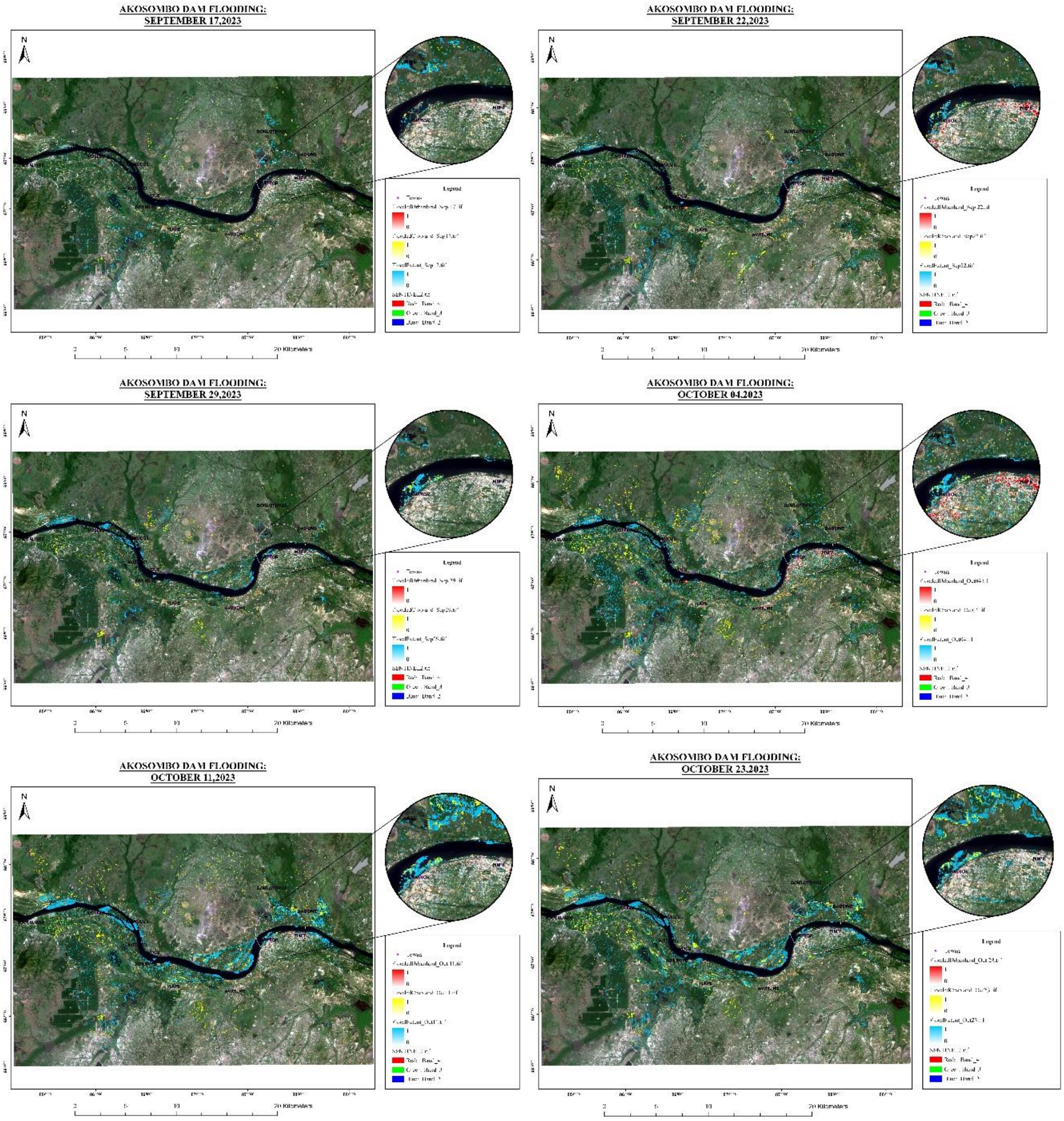

**AKOSOMBO DAM FLOODING:**
**OCTOBER 16,2023**

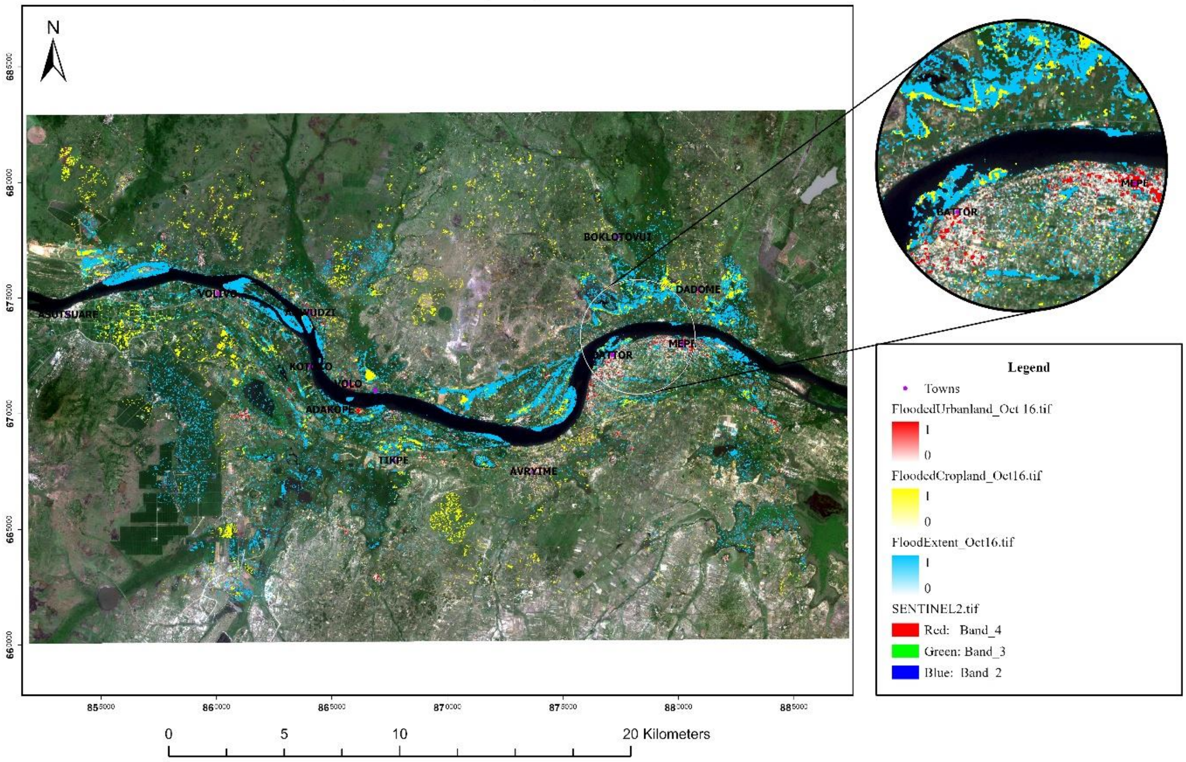


## 4.2 Analysis of Results

### Initial Flooding and Spillage Impact (September 17 - 22, 2023)

The spillage began on September 15, 2023, with a discharge rate of 20,000 cubic feet per second (cfs/day). By September 17, floodwater covered 802 hectares, including 139 hectares of cropland and 13 hectares of urban land. By September 22, the flooded area expanded to 1,246 hectares, with 201 hectares of cropland and 88 hectares of urban land submerged. The situation was concerning as the area of inundation grew, although it was largely confined to areas near the riverbanks.

### Rapid Expansion of Flooding (September 29 - October 11, 2023)

By September 27, the discharge rate had increased to manage the inflows into the reservoir, though exact figures for this date were not explicitly provided, leading to a significant escalation in flooding. On September 29, floodwaters expanded dramatically, covering 1,019 hectares of inundated area, including 194 hectares of cropland and 11 hectares of urban land. By October 4, the flood area surged to 2,407 hectares, severely impacting 467 hectares of cropland and 151 hectares of urban land. The expansion continued, with the flooded area reaching 2,458 hectares by October 11, submerging 438 hectares of cropland and 22 hectares of urban land.

**Peak and Recovery (October 16 - 23, 2023)**

By October 15, six spillage gates were opened to handle the overflow, maintaining the discharge at 183,000 cubic feet per second (cfs/day) to prevent overtopping of the dam. The flooding reached its peak on October 16, with 4,110 hectares inundated. This peak affected 753 hectares of cropland and 152 hectares of urban land, marking the most severe point of the flooding. Following this, by October 23, the floodwaters receded slightly, reducing the inundated area to 2,566 hectares, with 454 hectares of cropland and 12 hectares of urban land still submerged.

| DATES | INUNDATED AREAS | CROPLAND AREAS | URBAN LAND AREAS |
|---|---|---|---|
| 17-Sep | 802 | 139 | 13 |
| 22-Sep | 1246 | 201 | 88 |
| 29-Sep | 1019 | 194 | 11 |
| 4-Oct | 2407 | 467 | 151 |
| 11-Oct | 2458 | 438 | 22 |
| 16-Oct | 4110 | 753 | 152 |
| 23-Oct | 2566 | 454 | 12 |

## 4.3 Flood Hazard Score Analysis

The flood hazard score was derived through a multi-criteria analysis incorporating distance from water bodies, elevation, topographic position index (**TPI**), and wetness indices (**NDVI** and **NDWI**). The results are visualized in the accompanying maps, showing the distribution of flood hazard scores across the study area.

### 4.3.1 Distance from Water

Proximity to water bodies is a critical factor in determining flood risk. Areas closer to rivers and other water bodies are inherently more vulnerable to flooding. The distance was calculated using a fast distance transform algorithm, which provided a spatial representation of proximity to water bodies.

**High Risk (Score 5):** Areas within 250 meters of a water body were assigned the highest flood hazard score due to their extreme vulnerability.

**Moderate to Low Risk (Scores 1-4):** Regions further from water bodies, with distances ranging from 250 to over 1000 meters, received progressively lower hazard scores, indicating reduced flood risk. This map clearly shows the spatial distribution of flood hazards based on proximity to water bodies, with red zones representing the highest risk areas.

**DISTANCE HAZARD SCORE**

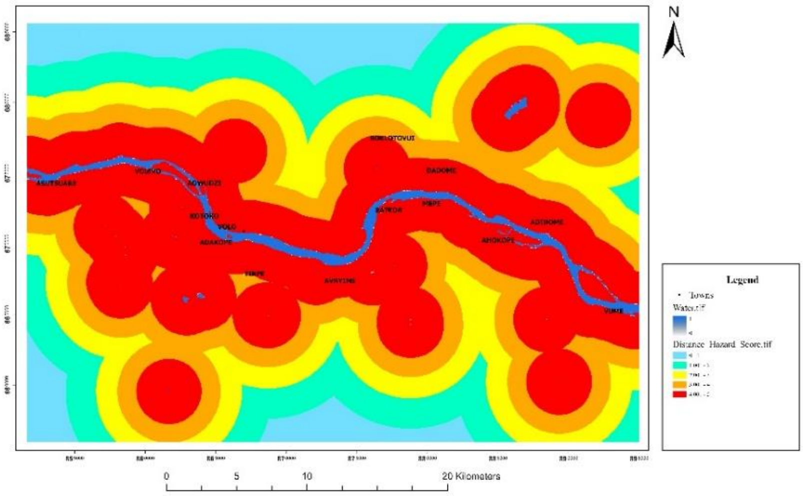


### 4.3.2 Elevation Hazard Score

Elevation is another crucial determinant of flood risk. Lower elevations are generally more susceptible to flooding due to the tendency of water to accumulate in low-lying areas.
**High Risk (Score 5):** Regions with elevations below 5 meters were classified as the highest flood risk areas.
**Moderate to Low Risk (Scores 1-4):** Higher elevations, ranging from 5% to above 20%, were assigned lower hazard scores, reflecting their decreased flood susceptibility.

**ELEVATION HAZARD SCORE**

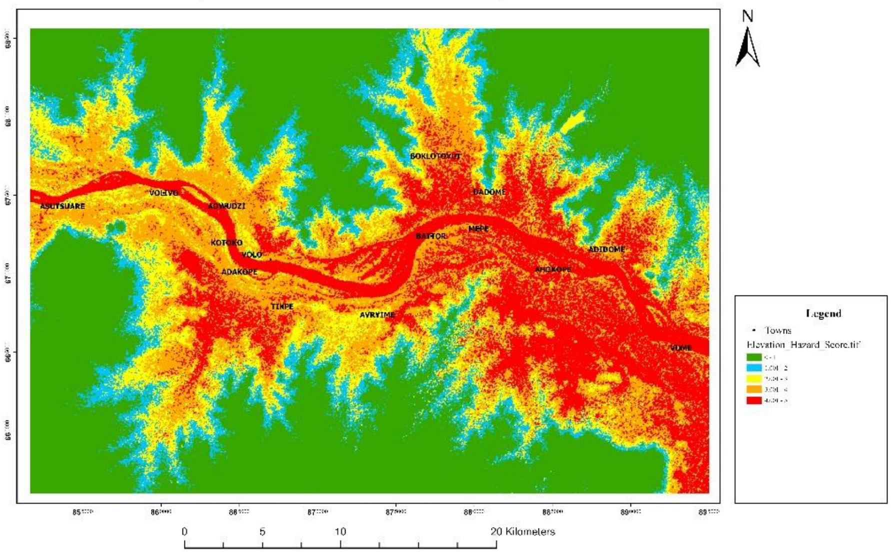

### 4.3.3 Flood Hazard Score

To create a comprehensive flood hazard map, the distance, elevation, TPI, and wetness indices were integrated. This approach allowed for a nuanced understanding of flood risk, taking into account multiple contributing factors.

**High Risk Areas (Score 5):** These areas, shown in dark red, are both low-lying and close to water bodies with poor drainage and high wetness indices, indicating severe flood risk.

**Moderate to Low-Risk Areas (Scores 1-4):** Represented in yellow, orange, and green, these areas have better drainage, higher elevations, and are farther from water bodies, making them less vulnerable to flooding.

Based on the flood hazard scores, safe havens were strategically identified and mapped to provide refuge for residents in high-risk areas. These safe havens were selected to ensure accessibility for towns most vulnerable to flooding.

A proximity analysis was conducted to determine the nearest safe havens for towns affected by the Akosombo Dam spillage. The analysis is crucial for planning effective evacuation strategies and ensuring that vulnerable populations have timely access to safe locations.

| Towns | Safe Haven | Nearest Distance |
|---|---|---|
| VUME | Safe Haven 9 | 6713.79854 |
| ADIDOME | Safe Haven 6 | 2304.216992 |
| DADOME | Safe Haven 7 | 1565.249728 |
| BOKLOTOVUI | Safe Haven 7 | 3361.883522 |
| MEPE | Safe Haven 7 | 3925.407884 |
| AHOKOPE | Safe Haven 5 | 4183.544861 |
| BATTOR | Safe Haven 8 | 5250.197747 |
| VOLO | Safe Haven 2 | 4159.807723 |
| AOWUDZI | Safe Haven 2 | 4735.072233 |
| AVRYIME | Safe Haven 4 | 3234.527413 |
| KLEBETIKOPE | Safe Haven 2 | 3616.240084 |
| VOLIVO | Safe Haven 3 | 3944.917177 |
| ASUTSUARE | Safe Haven 1 | 3573.522292 |
| KOTOKO | Safe Haven 2 | 5130.618596 |
| ADAKOPE | Safe Haven 2 | 5498.171848 |
| TIKPE | Safe Haven 10 | 3161.949577 |

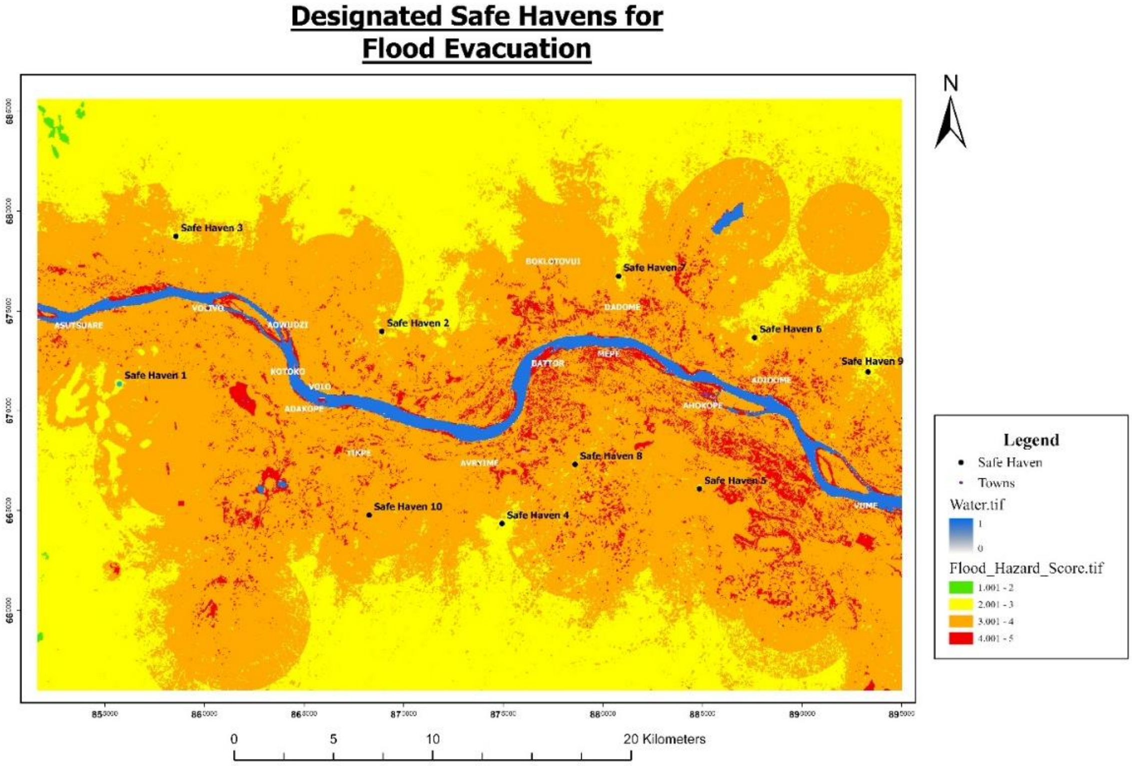


### 4.4 Discussions

The spillage of the Akosombo Dam and the subsequent flooding have significant implications for disaster management, agricultural stability, and urban planning. The extent of the flooding highlights vulnerabilities in various sectors, necessitating a multi-faceted approach to mitigate future risks. Addressing these challenges requires improved forecasting, resilient infrastructure, and better disaster preparedness strategies to safeguard communities and the economy.

**Implications of Findings**

One of the most affected sectors was agriculture, as floodwaters submerged 753 hectares of cropland by October 16. This prolonged exposure led to significant crop losses, threatening food security in the affected regions. Given the recurring nature of such events, there is an urgent need for improved flood forecasting and early warning systems to help farmers prepare for potential disasters.

Urban infrastructure was also severely impacted by the floods, with the affected land area increasing from 13 hectares on September 17 to 152 hectares by October 16. Future developments in flood-prone areas must prioritize flood-resistant designs, improved drainage systems, and updated building codes to minimize the impact of similar events.

Furthermore, the findings reveal gaps in disaster preparedness and response mechanisms. The sharp increase in flood-affected areas suggests that existing systems were not fully equipped to handle such abrupt changes. Enhancing contingency plans, implementing pre-emptive evacuations, and ensuring efficient resource deployment are essential to improving response efforts. Given these challenges, reassessing water management practices at the Akosombo Dam is crucial to balancing energy production with the potential downstream impacts of spillage.

Relevance to Disaster Management

The findings from this study provide valuable insights for improving disaster management, especially in flood-prone regions. The integration of remote sensing data with flood hazard scoring in Google Earth Engine (GEE) demonstrates the potential of geospatial technologies in enhancing flood preparedness and response efforts.

One key improvement lies in the development of enhanced early warning systems. By leveraging Sentinel-1 SAR imagery, authorities can monitor flood dynamics in near real-time, allowing for timely evacuations and targeted interventions to reduce loss of life and property.

Spatial analysis of flood impacts also plays a crucial role in disaster management. Identifying vulnerable regions through flood hazard mapping can inform land-use planning and infrastructure development, ensuring that new projects are designed to withstand flooding events.

## 4. CONCLUSSION AND RECOMMENDATIONS

### 4.1 Conclusion

The study successfully demonstrated that Sentinel-1 SAR data is highly effective in accurately detecting and mapping the extent of flooding caused by the Akosombo Dam spillage. The multi-temporal analysis allowed for precise monitoring of the flood progression over time, providing critical insights into the inundation dynamics. The impact assessment revealed significant damage to both agricultural lands and urban areas downstream of the dam. Floodwaters submerged extensive croplands, leading to potential long-term economic losses and food insecurity. Urban areas also suffered infrastructural damage, which disrupted local economies and displaced thousands of residents. The findings underscore the importance of proactive flood management practices, including the use of advanced remote sensing technologies for real-time monitoring. The study also suggests the need for further research into socio-economic resilience and adaptive capacity, particularly in communities most affected by dam spillage events.

### 4.2 Recommendation

**Strengthening Flood Monitoring and Early Warning Systems**

- **Real-time Monitoring Implementation:** Establishing real-time flood monitoring systems using a combination of satellite data and ground sensors can provide immediate insights during flood events, enabling proactive and timely responses.
- **Enhancement of Early Warning Mechanisms:** Developing robust early warning systems that integrate remote sensing data with meteorological forecasts can improve preparedness and reduce the adverse impacts of sudden flooding.

**Enhancing Flood Risk Management Strategies**

- **Integrated Flood Management Plans:** Formulating comprehensive flood management plans that incorporate structural measures (e.g., levees, dams) and non-structural measures (e.g., land-use planning, ecosystem restoration) can mitigate flood risks effectively.
- **Risk-sensitive Land-use Planning:** Authorities should enforce land-use policies that discourage development in high-risk flood zones and promote sustainable land management practices.
- **Infrastructure Resilience Building:** Investing in the design and construction of resilient infrastructure capable of withstanding flood events will reduce damage and facilitate quicker recovery.

**Promoting Community Awareness and Preparedness**

- **Public Education Campaigns:** Implementing continuous education and awareness programs can inform communities about flood risks, safety measures, and emergency procedures.
- **Community Engagement Initiatives:** Encouraging active participation of local communities in disaster planning and response can enhance resilience and ensure that strategies are tailored to specific local needs and contexts.

## REFERENCES

Ali, I., Cao, S., Naeimi, V., Paulik, C., & Wagner, W. (2018). Methods to Remove the Border Noise from Sentinel-1 Synthetic Aperture Radar Data: Implications and Importance For Time-Series Analysis. *IEEE Journal of Selected Topics in Applied Earth Observations and Remote Sensing*, *11*(3), 777–786. https://doi.org/10.1109/JSTARS.2017.2787650

Miescher, S. (2023). *Ghana: The Akosombo Dam disaster reveals a history of negligence that continues to this day*. UNDRR, Prevention Web. https://www.preventionweb.net/news/ghana-akosombo-dam-disaster-reveals-history-negligence-continues-day

Notti, D., Giordan, D., Caló, F., Pepe, A., Zucca, F., & Galve, J. P. (2018). Potential and Limitations of Open Satellite Data for Flood Mapping. *Remote Sensing*, *10*(11), 1673. https://doi.org/10.3390/rs10111673

Podest, E., & Mccartney, S. (2019). *National Aeronautics and Space Administration SAR for Flood Mapping using Google Earth Engine*.

Schlaffer, S., Chini, M., Giustarini, L., & Matgen, P. (2017). Probabilistic mapping of flood-induced backscatter changes in SAR time series. *International Journal of Applied Earth Observation and Geoinformation*, *56*, 77–87. https://doi.org/10.1016/j.jag.2016.12.003

*The Akosombo Dam Spillage | UNICEF Ghana*. (2023). https://www.unicef.org/ghana/blog/akosombo-dam-spillage

Vanama, V. S. K., Mandal, D., & Rao, Y. S. (2020). GEE4FLOOD: rapid mapping of flood areas using temporal Sentinel-1 SAR images with Google Earth Engine cloud platform. *Journal of Applied Remote Sensing*, *14*(03), 1. https://doi.org/10.1117/1.JRS.14.034505

## BIOGRAPHICAL NOTES

Bleboo Angela Bubune is a recent graduate of Geomatic Engineering at Kwame Nkrumah University of Science and Technology in Ghana. Her research interest lies in remote sensing and GIS. She is a member of the Ghana Institution of Surveyors Students' Society, where she served as the President. Currently, she is undertaking her national service at Soko Aerial Robotics and STS Centre For Research.

Kponor Mark Kofi is a recent graduate of Geomatic Engineering at Kwame Nkrumah University of Science and Technology, Ghana. He is currently undertaking his National Service at the Ghana Space Science and Technology Institute (GSSTI). His research interests focus on remote sensing using Earth Engine, Digital Earth Africa, and geospatial analysis for disaster management and environmental monitoring.

## CONTACT INFORMATION

Name: Angela Bleboo Bubune
Institution: Soko Aerial Robotics, Ghana Armed Forces
Address: 41 Defence Regiment, Burma Camp Accra
Telephone: (+233)594-678-124
Email: angelbubu2020@gmail.com

Name: Kponor Mark Kofi
Institution: Ghana Space Science and Technology Institute (GSSTI)
Address: P.O. Box LG 80, Legon
Telephone: (+233)546-509-680
Email: markkponor2916920@gmail.com
Website: **www.gssti.org**